Appendix B

Systematic Errors

B.1 Theoretical uncertainties

The simulation of events at the LHC is complex and can be conventionally divided into different parts which either involve the description of the interesting physics process or the description of the initial scattering conditions and the physics environment.

The simulation of the hardest part of the physics process is done via matrix element (ME) calculations at a certain order in the coupling constants and continues with the parton showering (PS) of the resulting partons until a cut-off scale, over which the perturbative evolution stops and the fragmentation of the final partons takes on. This cut-off is often referred to as factorisation scale, because it is the scale at which the two processes (showering and fragmentation) are supposed to factorise.

The interesting event is accompanied by the so-called underlying event (UE), term which identifies all the remnant activity from the same proton-proton (p-p) interaction and whose definition often includes ISR as well, and the pile-up, composed by other minimum bias (MB) p-p interactions in the same bunch crossing (up to 25 at high luminosity at the LHC). Moreover, since the initial state is not defined in p-p collisions, a proper description of the proton parton density functions (PDFs) should be included in the calculations.

Each of these effects needs to be modelled to the best of our knowledge, and the associated uncertainties need to be determined and propagated to the physics measurements. Moreover, many of the sources are correlated: for instance, fragmentation and showering are obviously dependent on each other, and in turn they assume a certain description of the underlying event. The task of assessing systematics due to theory and modelling can therefore be a difficult one and can sometime contain a certain degree of arbitrariness.

In what follows we propose some guidelines for the estimation of errors coming from the above, trying to divide the systematics sources into wider categories as much uncorrelated as possible: QCD radiation, fragmentation description, PDFs, UE and MB.

In attributing systematic errors we believe that one should use motivated recipes, avoiding unrealistic scenarios which will lead to unnecessarily conservative errors or, much worse, totally arbitrary assumptions.

B.1.1 Hard process description and parametric uncertainties

The description of the hard process should be done with Monte Carlo tools which are best suited to the specific analysis. For instance, when precise description of hard gluon emis-

sion becomes an issue, then next-to-leading order (NLO) generator tools like MC@NLO [770], or higher leading order (LO) α_s generators like COMPHEP [43], MADGRAPH [80], ALPGEN [160], and SHERPA [193] should be considered. This is in general true for both the signal and the background description.

When adopting a ME tool, one should always keep in mind that its output is often (if not always) supposed to be interfaced to PS Monte Carlo such as HERWIG [195], PYTHIA [24] or ISAJET [672], that treat the soft radiation and the subsequent transition of the partons into observable hadrons. One of the most difficult problems is to eliminate double counting where jets can arise from both higher order ME calculations and from hard emission during the shower evolution. Much theoretical progress has been made recently in this field [771–774]. For what concerns the ME/PS matched description of multi-jet final states, a rich spectrum of processes is currently available in ALPGEN. However, adopting general purpose generators like PYTHIA can still be the best option for topologies that are better described in the Leading Logarithm Approximation (LLA), for instance in the case of two leading jets and much softer secondary jets. The two different descriptions should be regarded as complementary.

In general, a sensible choice for the selection of the best generation tools can be driven by the HEPCODE data base [775]. However, comparison between different generators is recommended whenever applicable.

Each analysis needs then to make sure that other important effects (e.g. spin correlations in the final state, NLO ME corrections to top decays) are included in the generation mechanism. For example TOPREX [44], as long with some of the Monte Carlo generators already introduced in this section, provides a correct treatment of top quark spin correlations in the final state. Neglecting some of these effects corresponds to introducing an error in the analysis that cannot be considered as coming from a theoretical uncertainty.

For both signal and backgrounds, missing higher orders are a delicate source of uncertainty. Formally, the associated error cannot be evaluated unless the higher order calculation is available. This is often not possible, unless extrapolating by using comparisons with analytical calculations of total or differential cross-sections at the next order, if available. One should keep in mind that simple K-factors are not always enough and that the inclusion of higher orders typically also involves distortions in differential distributions.

Moreover, one should not forget that any Standard Model calculation is performed in certain schemes and that the input parameters are subject to their experimental uncertainties; if the error on most of those and the choice of the renormalisation scheme are expected to give negligible effects in comparison with other uncertainties, this might not be so for the choice of the hard process scale, which we will discuss in the next section, and some of the input parameters.

Among the input parameters, by far the one known with less accuracy will be the top mass. The current uncertainty of about 2% [776] enters in the LO calculations for processes which involve top or Higgs production. For instance, the total $t\bar{t}$ cross-section is known to have a corresponding 10% uncertainty due to this [45]. As far as Higgs production (in association or not with tops) is concerned, gluon-gluon fusion proceeds via a top loop and therefore the total cross-section can have a strong dependence on the top mass when $m_H \approx 2m_t$. Analyses which include Higgs bosons or top are encouraged to estimate the dependence of the significant observables on the top mass itself. Effects of m_t variation on acceptances of these analyses should instead be negligible.

B.1.2 Hard process scale

The hard process under study drives the definition of the Q^2 scale, which directly enters in the parametrisation of PDFs and α_s, hence in the expression of the cross sections.

The dependence of the observables on the choice for the Q^2 hard process scale is unphysical and should be regarded as one important contribution to the total uncertainty in the theoretical predictions. The sensitivity of the predicted observables to such choice is expected to decrease with the increasing order in which the calculation is performed, and can be tested by changing the hard process scale parameters in the generation (where applicable) using a set of sound values according to the characteristics of the hard process.

A sensible choice for the hard process scale in $2 \rightarrow 1$ processes is often $\hat{s}$, which is the default in general purpose generators like PYTHIA. Alternative choices to quote theoretical uncertainties can be $0.25\hat{s}$ and $4.0\hat{s}$. In PYTHIA this can be obtained acting on PARP(34).

For $2 \rightarrow n$ processes, many reasonable alternatives for the Q^2 scale definition exist. The PYTHIA default (MSTP(32)=8), corresponds to the average squared transverse mass of the outgoing objects. It is possible to test the sensitivity on the Q^2 scale switching to different options, for example trying $Q^2 = \hat{s}$ (MSTP(32)=4 in PYTHIA).

B.1.3 PDF description

The parton distribution functions of interacting particles describe the probability density for partons undergoing hard scattering at the hard process scale Q^2 and taking a certain fraction x of the total particle momentum. Since the Q^2 evolution can be calculated perturbatively in the framework of QCD, PDFs measurements can be cross checked using heterogeneous DIS, Drell-Yan and jet data, and achieve predictivity for points where no direct measurements are available yet, for example in a large region of the (x,Q^2) space for p-p interactions at the LHC energy.

Various approaches are currently available to quote the PDFs of the proton, which propose different solutions for what concerns the functional form, the theoretical scheme, the order of the QCD global analysis (including possible QED corrections), and the samples of data retained in the fits: CTEQ [777], MRST [778], Botje [779], Alekhin [780] etc. The CTEQ and MRST PDFs, including Tevatron jet data in the fits, seem to be well suited for use in Monte Carlo simulations for the LHC.

The best way to evaluate theoretical uncertainties due to a certain proton PDFs is to vary the errors on the parameters of the PDF fit itself. With the Les Houches accord [94] PDF (LHAPDF) errors should be easily propagated via re-weighting to the final observables. However, errors are available only for NLO PDF, whereas in most of the cases only LO tools are available for the process calculation. Correctly performing evaluation of theoretical uncertainties in these cases requires some care. The proposed solution is to adopt CTEQxL (LO) for the reference predictions using CTEQxM (NLO) only to determine the errors.

For analyses which are known to be particularly sensitive to PDFs, like cross-section measurements, it would be also desirable to compare two different sets of PDFs (typically CTEQ vs MRST) taking then the maximum variation as an extra error. This is important since, even considering the error boundaries, different set of PDFs may not overlap in some region of the phase space.

The LHAGLUE interface [94] included from the most recent LHAPDF versions simplifies the

use of the Les Houches accord PDF in PYTHIA by the switches MSTP(52) = 2 , MSTP(51) = LHAPDF$_{id}$.

B.1.4 QCD radiation: the parton shower Monte Carlo

The showering algorithm is basically a numeric Markov-like implementation of the QCD dynamic in the LLA. After the generation of a given configuration at partonic level, the initial state radiation (ISR) and the final state radiation (FSR) are produced following unitary evolutions with probabilities defined by the showering algorithm.

The probability for a parton to radiate, generating a $1 \rightarrow 2$ branching, are given by the Altarelli-Parisi equations [781], however various implementations of the showering algorithm exist in parton shower Monte Carlo, which mostly differ for the definition of the Q^2 evolution variable (virtuality scale) in the $1 \rightarrow 2$ radiation branching and for the possible prescriptions limiting the phase space accessible to the radiation: PYTHIA, HERWIG, ARIADNE [782], ISAJET etc.

The virtuality scales for both ISR and FSR need to be matched to the hard process scale, the latter setting an upper limit on the former ones; such limit has to be considered in a flexible way, given the level of arbitrariness in the scale definitions. While this matching is somewhat guaranteed if one adopts the same simulation tool for both hard scattering and parton shower, a careful cross check is recommended in all other cases. In general, a critical judgement taking into account the hard process type is needed. Allowing a virtuality scale higher than the hard process scale may give rise to double counting. This is the case of $gg \rightarrow gg$ processes with additional hard gluons added in the showering. However other processes are safer from this point of view, for instance the case of the $q\bar{q} \rightarrow Z$ process at LO.

Quantum interference effects in hadronic collisions have been observed by CDF [783] and DØ [784] studying the kinematical correlations between the third jet (regarded as the result of a soft branching in the LLA) and the second one. The implementation of the so called colour coherence in PS Monte Carlo is made in the limit of large number of colours and for soft and collinear emissions, restricting the phase space available to the radiation depending on the developed colour configuration. Different implementations of the colour coherence are available in HERWIG and PYTHIA, while ISAJET doesn't take into account such effects.

The theoretical uncertainty associated to the parton showering descriptions, includes what is normally referred to as ISR or FSR and their interference. In order to achieve practical examples for the recommended parton shower settings, we will consider PYTHIA as the default tool for showering from now on.

Turning OFF ISR and FSR (MSTP(61)=0, MSTP(71)=0 respectively) or even the interference part (MSTP(62)=0, MSTP(67)=0) is certainly a too crude approach and, to a large extent, a totally arbitrary procedure to assess a systematic error. We believe it is much more realistic to vary, according to sound boundaries, the switches regulating the amount and the strength of the radiation of the showering. These can correspond to $\Lambda_{\rm QCD}$ and the maximum virtuality scales up to which ISR stops and from which FSR starts. It would be important to switch the parameters consistently going from low to high values in both ISR and FSR.

Notice that the radiation parameters were typically fitted at LEP1 together with the fragmentation parameters, benefiting from a much simplified scenario where no ambiguity on the maximum virtuality scale applies, the only relevant energy scale of the problem being

$\hat{s} = s$. One has to take into account that while for instance FSR accompanying heavy boson decays at the LHC can be directly related to the LEP experience, FSR in processes like gg→b$\bar{\text{b}}$ entails additional uncertainties arising from the maximum allowed virtuality scale and ISR/FSR interference. On top of that, additional complications arise from the fact that ISR at hadron machines contributes to the description of the underlying event. Matching two different tunings of the same parameter (in particular PARP(67)) can be very subtle at the LHC.

These are the suggested settings in PYTHIA, which have been cross-checked with the ones adopted by the CDF experiment and also follow the prescription by the main author:

- $\Lambda_{\rm QCD}$: PARP(61), PARP(72), PARJ(81) from 0.15 to 0.35 GeV consistently, symmetric with respect to 0.25. Notice that these settings have been optimised for the CTEQ6L PDFs. In general different ranges apply when changing PDFs. In order to give the user full control on these parameters the option MSTP(3)=1 has to be set, otherwise $\Lambda_{\rm QCD}$ is assumed to be derived from the PDFs parametrisation.
- $\mathbf{Q}^2_{\rm max}$: PARP(67) from 0.25 to 4 and PARP(71) from 1 to 16 going from low to high emission in a correlated way. In doing so one should also make sure that the tuning of the underlying event is not changing at the same time. Possible retuning of the underlying event in different radiation scenarios may be needed, in particular for what concerns PARP(82).

B.1.5 Fragmentation

Perturbative QCD cannot provide the full description of the transition from primary quarks to observable hadrons, but only the part which involves large momentum transfer. The formation of final hadrons involves a range of interactions which goes above the Fermi scale and where the strong coupling constant $\alpha_{\rm s}$ increases above unity, making it necessary to describe this part in a non-perturbative way, normally referred to as fragmentation or hadronisation.

The non-perturbative description of fragmentation is realised via models, which need to be tuned to experimental data. The data correspond, typically, to event shapes and multiplicities at leptonic machines or to the inclusive jet shapes at hadronic machines. A comprehensive overview of the models can be found in [785].

Fragmentation is said to depend only on the factorisation scale if jet universality is assumed, i.e. assuming that jets fragment in the same way at hadron and lepton machines. Jet universality will be ultimately verified at the LHC; one should clarify whether instrumental effects and the LHC environment will have an impact on the final observables. For instance, the much larger fraction of gluon jets or the different description of the underlying event can change the values of the parameters that regulate the fragmentation. Moreover, for events with high multiplicity of jets it will also be crucial to properly describe fragmentation in conditions where large jet overlapping is to be expected and where inclusive tunings might not be ideal.

The consequence of jet universality is that, once the PS cut-off scale is fixed, the fragmentation description for light quarks should be universal, and the LEP/SLD tunings (or the Tevatron ones) could be used as they are for the LHC.

It is important to underline that the description of the non-perturbative part of the radiation also depends on the way the perturbative one is described. This means that one should not use a tuning of fragmentation done with LO(+LL) tools (typically PYTHIA at LEP) attached

to perturbative calculation which are done at higher -or different- order.

B.1.5.1 Light quarks fragmentation

In the absence of LHC data, the best choice is therefore to use a model tuned to the LEP and SLD data [786–788]. It is important to choose the tuning in a consistent way from the same experiment, given that a combined LEP/SLD tuning has never been attempted. As a possibility, suggested by the major success in describing the data and by its extensive use in the experimental collaborations, is the use of PYTHIA, which uses the string (or Lund) fragmentation model [789]. The parameters that we consider more relevant in PYTHIA for the description of fragmentation are the following, where the central value is taken by the fit performed by the OPAL Collaboration, as an example:

PARJ(81) = 0.250
PARJ(82) = 1.90
PARJ(41) = 0.11
PARJ(42) = 0.52
PARJ(21) = 0.40

where PARJ(81) ($\Lambda_{\rm QCD}$) and PARJ(82) ($Q^2_{\rm min}$) refer to the radiation part. To properly evaluate a systematic error due to pure fragmentation one should vary only PARJ(42) and PARJ(21) by their respective errors (0.04 and 0.03 for OPAL). The variation should account for the proper parameter correlation if the effect is critical for the analysis. PARJ(41) is totally correlated to PARJ(42).

Alternatively, or additionally, it would also be important to compare PYTHIA with HERWIG with consistent tunings from LEP [786–788]; in doing so it is important to factorise the UE description (see next section) that can induce important differences in the results.

B.1.5.2 Heavy quarks fragmentation

The description of the heavy quarks fragmentation is important for top physics and for those processes with large b production in the final states. Exclusive channels are particularly influenced by the description of the fragmentation of the b quark.

The description of the fragmentation of the heavy quarks has been tuned to Z data at LEP and SLD[787, 790–792] (via a measurement of $x_{\rm B}$ and $x_{\rm D}$) and $b\bar{b}$ data at the Tevatron, using different fragmentation functions like Lund, Bowler [793], Peterson [794], Kartvelishvili [795].

In the spirit of fragmentation universality the LEP/SLD tunings can be adopted for the LHC, but with much care. Significant differences among the fitted values in different experiment can point out that the factorisation scale used for the PS is not the same everywhere. One should make sure that the scale used is set consistently with the chosen fragmentation function parameters. This can be done by using the tuning from only one experiment, making sure to also use the main switches of the parton showering, (PARJ(81) and PARJ(82) in PYTHIA).

The fragmentation function that best describes heavy flavour data at LEP is Bowler. With the same OPAL tuning reported above the best fit of the Bowler parameters, a and $bm^2_\perp$, to data gives:

$bm_{\perp}^2 = 65^{+17}_{-14}$
$a = 15.0 \pm 2.3$

The Bowler model would extend the string model to heavy flavours, describing the corrections in terms of the charm and bottom masses. Unfortunately, no tuning exists in the literature which is capable to describe at the same time light and heavy quark fragmentation, i.e. adopting universal parameters a = PARJ(41) and b = PARJ(42) for both light and heavy quarks.

Alternatively, the widely used Peterson function can be used, and its parameters are directly switchable in PYTHIA for just b and c fragmentation:

PARJ(54) = -0.031 $\pm$ 0.011
PARJ(55) = -0.0041 $\pm$ 0.0004

where the two parameters correspond, respectively, to ϵ_{c} and ϵ_{b} fitted in the OPAL tuning. The systematic can then be evaluated by varying the errors on the fitted parameters or by comparing with a different fragmentation function like Kartvelishvili, or Lund.

An important feature of the b fragmentation that should be considered by those analyses in the top sector sensitive to the details of the fragmentation, is the way the b fragments in top decays. At the LHC the b from a t is hadronising with a beam remnant, introducing potentially worrying differences with respect to the fragmentation at LEP. The main effects are presented in [796] and are known as *cluster collapse*, happening when a very low mass strings quark-remnant directly produces hadrons without fragmenting, hence enhancing the original flavour content, and *beam drag*, which is an angular distortion of hadron distribution toward the end of the string in the remnant. If, under reasonable assumptions on the transverse momentum in top events at the LHC, one can exclude to a large extent the importance of the first effect, beam drag could potentially introduce B meson production asymmetries, even though estimations are keeping the effect at the level of 1% at the LHC [796].

B.1.6 Minimum bias and underlying event

Multiple parton interaction models, extending the QCD perturbative picture to the soft regime, turn out to be particularly adequate to describe the physics of minimum bias and underlying event. Examples of these models are implemented in the general purpose simulation programs PYTHIA, HERWIG/JIMMY [192], and SHERPA. Other successful descriptions of underlying event and minimum bias at hadron colliders are achieved by alternative approaches like PHOJET [797], which rely on both perturbative QCD and Double Pomeron Models (DPM).

Huge progress in the phenomenological study of the underlying event in jet events have been achieved by the CDF experiment at Tevatron [798], using the multiplicity and transverse momentum spectra of charged tracks in different regions in the azimuth-pseudorapidity space defined with respect to the direction of the leading jet. Regions that receive contributions only by the underlying event have been identified. The average charged multiplicity per unit of pseudorapidity in these regions turns out to be significantly higher with respect to the one measured in minimum bias events. This effect, referred to as "pedestal effect", is well reproduced only by varying impact parameters models with correlated parton-parton interactions (MSTP(82)>1 in PYTHIA). Simpler models are definitely ruled out.

The main problem of extrapolating the predictions of the multiple interactions models to the LHC is that some of the parameters are explicitly energy dependent, in particular the colour screening p_T cut-off (PARP(82) at the tuning energy PARP(89) in PYTHIA). The CDF tuning, often referred to as Tune-A, is not concentrating on this particular aspect. Other works [196, 799] have put more emphasis on this issue. However, one of their results is that currently only PYTHIA can be tuned to provide at the same time description of CDF and lower energy minimum bias data from UA5. One of these tunings can be summarised as follows:

PARP(82) = 2.9
PARP(83) = 0.5
PAPR(84) = 0.4
PARP(85) = 0.33
PARP(86) = 0.66
PARP(89) = 14000
PARP(90) = 0.16
PARP(91) = 1.0
MSTP(81) = 1
MSTP(82) = 4

Sensible estimation of theoretical uncertainties arising from underlying event and minimum bias modelling can be performed assigning $\pm 3\sigma$ variations to the colour screening p_T cut-off parameter tuned on minimum bias CDF and UA5 data and extrapolated to the LHC energy [799], i.e. varying PARP(82) in the range [2.4-3.4], while keeping the other parameters listed above to their tuned values.

As a new tool for the description of UE and MB we would like to mention PYTHIA 6.3 [800], that allows for new interesting features, including the new p_T-ordered initial- and final-state showers and a new very sophisticated multiple interactions model that achieves description of colliding partons in the proton in terms of correlated multi-parton distribution functions of flavours, colours and longitudinal momenta. However, as stressed by the PYTHIA authors, the new model (PYEVNW) is still not so well explored. Therefore the old model (PYEVNT) is retained as the default choice, with full backward compatibility. Moreover, in the use of PYTHIA 6.3, one should be careful when switching to the new p_T-ordered showers and multiple interaction models, as their parameters are not tuned yet, in particular for what concerns the energy dependence, necessary to get meaningful extrapolations at the LHC energy.

B.1.7 Pile-up and LHC cross sections

The design parameters of the LHC at both low and high luminosity are such that, on top of possible signal events, additional minimum bias interactions are produced in the same beam crossing, the so-called Pile-up effect.

Pile-up is a purely statistical effect. The number of minimum bias interactions generated in a single beam crossing is a Poissonian distribution that depends on the instantaneous luminosity, which varies of about a factor 2 during a LHC fill. Although luminosity variation is not arising from theoretical uncertainties, it is recommended to cross check the stability of the results against variation of the nominal luminosity.

An issue which can affect the Pile-up is the definition of the minimum bias itself. The latter, indeed, may or may not include the diffractive and elastic contributions, with figures for the total cross section which can vary from 100 mb to 50 mb respectively. If the PYTHIA generator is adopted, these two different options correspond to MSEL 2 and MSEL 1, however, in order to get full control on the different contributions to the cross sections, one can use MSEL 2, setting MSTP(31) = 0, and providing explicit input through SIGT(0,0,J), where the meaning of the index J is described below:

J=0 Total cross section (reference value = 101.3 mb).

J=1 Elastic cross section (reference value = 22.2 mb).

J=2 Single diffractive cross section XB (reference value = 7.2 mb).

J=3 Single diffractive cross section AX (reference value = 7.2 mb).

J=4 Double diffractive cross section (reference value = 9.5 mb).

J=5 Inelastic, non-diffractive cross section (reference value = 55.2 mb).

Where J=0 has to correspond to the sum of the contributions for J=1,...,5. With respect to alternative cross section predictions [801], PYTHIA reference values for diffractive cross sections might be slightly shifted on the high side. A possible sound alternative could be to reduce the diffractive cross sections of around 30%, keeping constant the total cross section.

In order to assess the sensitivity of one analysis to the diffractive variations in the pile-up, at least the two options MSEL 1 and MSEL 2 should be tried. Diffractive contribution will in general result in few additional soft charged particles spiraling in the high magnetic fields of the LHC experiments. This effect is most likely to be relevant in the tracker detectors, where multiple hits in the same layer can be generated by the same track.

B.1.8 Decays

In contrast to the simple decay models available in the common PS Monte Carlo, alternative hadron decay models exist, for example EVTGEN [802], which have huge collections of exclusive hadron decays up to branching ratios as low as 10^{-4}.

EVTGEN follows the spin density matrix formalism and has an easily tuneable and upgradeable hadron decay data base which currently constitutes the largest and most refined collection of hadron decay models.

Comparison between the simple default decay models implemented in PS Monte Carlo and those available in EVTGEN should be recommended at least for analyses dealing with B hadrons or relying on b-tagging. However, since switching to a new hadron decay model could have a deep spin-offs on the exclusive description of the final states (multiplicity of kaons, pions, photons and muons, multiplicity of tracks reconstructed in secondary vertices) it might be worth to study also effects on trigger performances.

The LHC version of EVTGEN was initially provided by the LHCb experiment and is currently maintained by LCG Generator [803]. It comprises an interface to PYTHIA simulation that solves the technical problems of switching between the two different scenarios (i.e. hadron decays performed by PYTHIA, hadron decays performed by EVTGEN).

B.1.9 LHAPDF and PDF uncertainties

The detailed investigations of processes at LHC required a well understanding of the systematic theoretical uncertainties [200]. One of the important source of such errors is the parton distribution functions (PDFs).

The Les Houches Accord Parton Density Functions (LHAPDF) package [94] is designed to work with the different PDF sets *. In this approach a "fit" to the data is no longer described by a single PDF, but by a PDF set consisting of many individual PDF members. Indeed, PDFs are specified in a parameterised form at a fixed energy scale Q_0, such as

$$f(x, Q_0) = a_0 x^{a_1}(1-x)^{a_2}(1 + a_3 x^{a_4}...) \tag{B.1}$$

The PDFs at all higher Q are determined by NLO perturbative QCD evolution equations. The total number of PDF parameters (d) could be large (for example, for CTEQ parametrisation one has $d = 20$ [12]). Fitting procedure is used for evaluation an effective χ^2 function, which can be used to extract the "best fit" (the global minimum of χ^2) and also to explore the neighbourhood of the global minimum in order to quantify the uncertainties. As a result one has the "best-fit" PDF and $2d$ subsets of PDF [12, 94]:

$$f_0(x, Q),\ f_i^{\pm}(x, Q) = f\left(x, Q;\ \{a_i^{\pm}\}\right),\ \ i = 1, ..., d \tag{B.2}$$

B.1.9.1 Master equations for calculating uncertainties

Let $X(\{a\})$ be any variable that depends on the PDFs. It can be a physical quantity such as the W production cross section, or a differential distribution.

Let $X_0 = X(\{a_0\})$ be the estimate for X calculated with the best-fit PDF and $X_i^{\pm}$ be the observable X calculated with i-th subset $f_i^{\pm}(x, Q)$.

Following to CTEQ6 collaboration one can estimate the variation of X by using a master formula [12]:

$$\Delta X = \sqrt{\sum_{i=1}^{d} \left(X_i^+ - X_i^-\right)^2} \tag{B.3}$$

However, very often many X_i^+ and X_i^- have different magnitudes and even signs ! This failure of the master formula is a result of the simple observation that the PDF set that minimises the uncertainty in a given observable X is not necessarily the same as the one that minimises the fit to the global data set.

The better estimator for the uncertainty of a generic observable X was proposed in [804]. It is defined as the maximum positive and negative errors on an observable X by

$$\left.\begin{aligned} \Delta X_+ &= \sqrt{\textstyle\sum_{i=1}^{d} \left(\max[(X_i^+ - X_0),\ (X_i^- - X_0)\,,\ 0]\right)^2}, \\ \Delta X_- &= \sqrt{\textstyle\sum_{i=1}^{d} \left(\max[(X_0 - X_i^+),\ (X_0 - X_i^-)\,,\ 0]\right)^2} \end{aligned}\right\} \tag{B.4}$$

*Note, at CMS it was recommended to use the CTEQ 5L set for PTDR simulation. Since there is only **one** CTEQ 5L PDF set (without corresponding subsets), it was recommended to use CTEQ 6M for evaluation of uncertainties due to PDFs for PTDR estimates and only in a special case one can use another sets (e.g. MRST).

In Eqs. (B.4) one sums the maximum deviations on the observable in each of the parameter directions, and hence retain both maximal sensitivity to the parameters that vary most and estimate the range of allowed values of the cross section. Note, that the errors in Table C.2 were evaluated with this Eq. (B.4).

Eq. (B.4 could also be used for calculations of differential distribution. Fig. B.1 presents the differential distribution $d\sigma/dP_T$ for $t\bar{t}$-pair production at LHC.

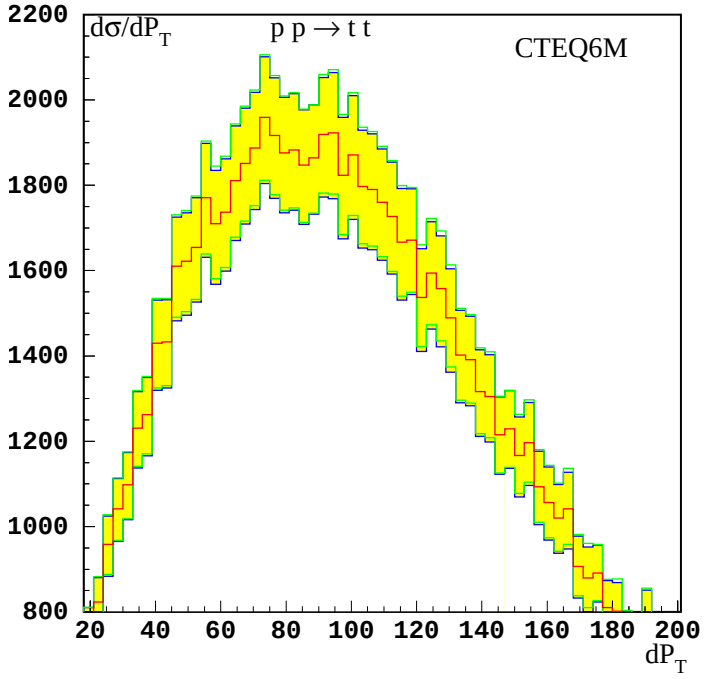

Figure B.1: $d\sigma/dP_T$ distribution for $t\bar{t}$-pair production at LHC. The central histogram corresponds to the 'best-fit' of CTEQ6M PDF, while the shaded area represents the deviation due to PDF uncertainties.

B.1.9.2 How to calculate $X(\{a_i\})$?

The most simple and straightforward method is to simulate a sample with the "best-fit" PDFs and then to repeat a such simulation $2d$ times with different $2d$ PDF subsets. As a results one gets $(1+2d)$ samples of **unweighted** events with **different** kinematics for each samples. Then use these samples to calculate $(1+2d)$ values for observable:

$$X_0 = \sum_{\text{events}} X_n(\{a_0\})), \quad X_i^{\pm} = \sum_{\text{events}} X_n(\{a_i^{\pm}\}), \quad i = 1, ..., d \tag{B.5}$$

In practice, such method requires a large CPU-time and can be recommended only to be used for very few special cases, when a high accuracy is required.

In the second approach (**"re-weighting" method**) one needs to simulate only **one** sample with the 'best-fit' PDF. In doing so the additional weights, corresponding to all other PDF subsets are evaluated. This weight is the ratio of the parton luminosity [PDF$(\{a_i\})$ – the product of PDFs] evaluated with PDF subset to the parton luminosity, calculated with the 'best-fit' PDF. As a result, for any n-event one has $2d$ additional weights:

$$w_{(0)} = 1(\text{best fit PDF}), \quad w_{(i)}^{\pm} = \frac{\text{PDF}(\{a_i^{\pm}\})_n}{\text{PDF}(\{a_0\})_n}; \quad w_{(i)}^{\pm} = \mathcal{O}(1) \tag{B.6}$$

The corresponding $(1+2d)$ values for observable X are evaluated as follows:

$$X_0 = \sum_{\text{events}} X_n(\{a_0\})), \;\; X_i^{\pm} = \sum_{\text{events}} w_{(i)}^{\pm} X_n(\{a_0\}) \tag{B.7}$$

Contrary to the first method (see (B.5)) these $(1+2d)$ samples have the events with **different** weights, but with **identical** kinematics for each samples. Note, that all additional samples have different "total number of events":

$$N_0 = \sum_{\text{events}} w_{(0)}(=1), \; N_i^{\pm} = \sum_{\text{events}} w_{(i)}^{\pm} \neq N_0, \text{ and } N_i^{\pm} = \mathcal{O}(N_0) \tag{B.8}$$

Starting from CMKIN_6_0_0 version it is possible for each event the evaluation of the additional weights, corresponding to different PDF subsets (i.e. $w_{(i)}^{\pm}$, see (B.6)). This option is available for CMKIN run with PYTHIA-like generators (PYTHIA, MADGRAPH, COMPHEP, ALPGEN, TOPREX, STAGEN, etc) and HERWIG. This information is written in `/mc_param/` user block after all variables filled by CMKIN and a user (by using of `kis_xxx` routines).

B.2 Experimental uncertainties

The systematic uncertainties associated with the detector measurements contributing to an analysis are mostly covered in the corresponding chapters of Volume 1 of this Report [7] and are summarised here.

B.2.1 Luminosity uncertainty

As discussed in Chapter 8 of [7], the design goal for the precision of the luminosity measurement at CMS is 5%, which is assumed to be achieved after 1 fb^{-1} of data has been collected. For integrated luminosities of less than 1 fb^{-1}, it is assumed that the precision is limited to 10%. For studies based on 30 fb^{-1} or more in this Report, it is assumed that further improvement on the uncertainty can be achieved and a 3% uncertainty is assumed, via e.g. W,Z based luminosity measurements.

B.2.2 Track and vertex reconstruction uncertainties

The uncertainty in the silicon track reconstruction efficiency is taken to be 1% for all tracks. The primary vertex precision along the z coordinate is expected to be about 10 μm once 1 fb^{-1} has been collected. The transverse vertex precision is expected to be about 1 μm.

The effects of uncertainties on the alignment of silicon sensors on track and vertex reconstruction are studied using a dedicated software tool (Section 6.6.4 of [7]) that is able to displace tracker elements according to 2 scenarios: a "First Data Taking Scenario" with placement uncertainties as expected at LHC start-up from measurements using the laser alignment system for the strip tracker and from in-situ track-based alignment of the pixel detector, and a "Long Term Scenario" appropriate after the first few fb^{-1} have been collected and a complete track-based alignment has been carried out for all tracker elements.

The effect of the magnetic field uncertainty in the central region of CMS is expected to contribute a momentum scale uncertainty of 0.0003 GeV/c to $1/p_{\mathrm{T}}$. When combined with the aggregate effect from alignment uncertainties, the overall momentum scale uncertainty is 0.0005 GeV/c at start-up.

B.2.3 Muon reconstruction uncertainties

As with the silicon tracker studies, a dedicated software tool has been developed (Section 3.2.2 of [7]) to study the effects of muon detector placement uncertainties on muon reconstruction. Two scenarios, a "First Data Taking Scenario" with placement uncertainties as expected at LHC start-up and a "Long Term Scenario" appropriate after the first few fb^{-1}, are available and used in analyses sensitive to the alignment precision of the muon detectors. The latter scenario describes a detector alignment precision of 200 μm in the plane transverse to the beam axis using the laser alignment system and track-based alignment strategies.

The effect of magnetic field uncertainties on the muon momentum will be dominated by the uncertainty in the central region and its impact on the momentum scale determined by fits to the silicon tracker hits for muon momenta well below the TeV/c scale.

B.2.4 Electromagnetic calibration and energy scale uncertainties

The precision to which the ECAL crystals can be intercalibrated from a variety of techniques is discussed in Section 4.4 of [7], and ranges from 0.4–2.0% using about $5\,\mathrm{fb}^{-1}$ of in-situ single isolated electron data. A software tool is used to apply calibration constants to the accuracy expected to be obtained with either $1\,\mathrm{fb}^{-1}$ or $10\,\mathrm{fb}^{-1}$ of integrated luminosity. The absolute energy scale can be determined using the Z mass constraint in $\mathrm{Z} \to \mathrm{ee}$ decays, and is expected to be measured to a precision of about 0.05%.

B.2.5 Jet and missing transverse energy uncertainties

The estimated systematic uncertainty on the jet energy scale is shown in Fig. B.2. At startup the accuracy of the jet energy scale relies on the understanding of single-particle test beam calibration and the level of agreement achieved in the data-to-Monte Carlo simulation comparisons of the detector response. The response of an individual tile or crystals is known to limited accuracy from source calibration in the HCAL and test stand measurements for crystals in the ECAL. Hence, given the limitations of the precalibration of the calorimeters, an overall uncertainty of 15% is expected for the "day-one" absolute energy scale. This applies equally for jet response and the energy scale uncertainty of the missing transverse energy.

In the first 1–10 fb^{-1} of data, the γ+jet calibration [282] and the hadronic W boson mass calibration in top quark pair production events [286] are currently the best estimates for the accuracy on the absolute jet energy scale. The hadronic W jets in the selected sample have a mean p_{T} that is approximately 50 GeV/c. A lowering of the jet selection threshold increases the effects of the offset correction from pile-up. The systematic on offset corrections and backgrounds puts the absolute jet energy scale at 3%. The jet reconstruction efficiencies are flat above 50 GeV/c, but drop in the low p_{T} region. The current estimate of the high p_{T} jet energy scale based on the hadronic W calibration is 3%. The calorimeter response curves that are required to extrapolate to high p_{T} are not expected to significantly increase the energy scale uncertainty beyond the 3% from the W calibration. In the low p_{T} region excluded from the hadronic W analysis, the absolute jet energy scale will be set by the γ+jet calibration which will extend down to 20 GeV. Below 20 GeV, only the single-particle calibration methods apply and these will have an accuracy of 10%. The recommended treatment for the jet

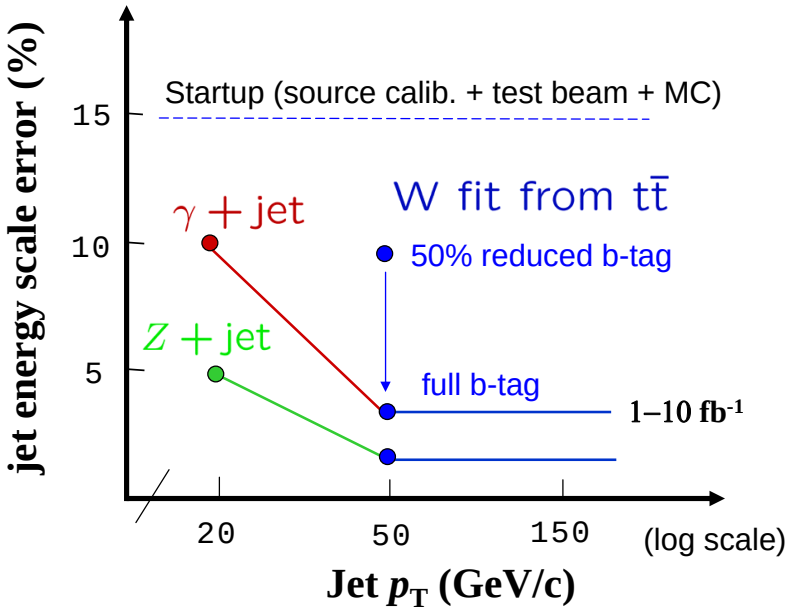

Figure B.2: Jet energy scale uncertainty is applied as a rescaling of the four-momentum of the reconstructed jet $p^{\mu,jet}_{scaled\pm} = (1 \pm \alpha) \cdot p^{\mu,jet}_{meas}$ where α is the percentage uncertainty plotted above.

energy systematic in this report is to apply an uncertainty according to this functional form:

$$\sigma^{jet}_E/E = \begin{cases} 10\% & p_{\mathrm{T}} < 20\,\mathrm{GeV/c} \\ 10\% - 7\% * (p_{\mathrm{T}} - 20\,\mathrm{GeV/c})/(30\,\mathrm{GeV/c}) & 20\,\mathrm{GeV/c} < p_{\mathrm{T}} < 50\,\mathrm{GeV/c} \\ 3\% & p_{\mathrm{T}} > 50\,\mathrm{GeV/c} \end{cases}$$

It is expected that the Z+jet sample and further analysis of the hadronic W systematics will reduce the overall jet energy scale uncertainty, but these analyses remain under active study.

The low p_{T} region is particularly important for the missing transverse energy (MET) response. As the MET will have significant contributions from low p_{T} jets and unclustered energy, it is expected that the low p_{T} component of the MET will not be understood to better than 10% following the first 1–10 fb^{-1} of data. The recommended treatment of the MET energy scale uncertainty has two approaches (one simple and one more detailed). For a MET which is known to be dominated by low p_{T} jets and unclustered energy, an uncertainty of 10% should be applied to the components of the MET uncorrelated to the jet energy scale uncertainty of the jets. This is the simple approach and gives a conservative error on the MET. For events with reconstructed high p_{T} jets, the contributions to the MET uncertainty are correlated to the jet energy scale uncertainty of the high p_{T} jets. The recommended treatment of the MET uncertainty is to apply separate uncertainties on the low p_{T} and high p_{T} components of the MET. The MET is reconstructed as described in [146] and [147]. This gives a type-1 correction of the following form:

$$E^{\mathrm{miss}}_{\mathrm{Tx(y)}} = -\left[E^{\mathrm{raw}}_{\mathrm{Tx(y)}} + \sum_{\mathrm{jets}} \left(p^{\mathrm{corr.\ jet}}_{\mathrm{Tx(y)}} - p^{\mathrm{raw\ jet}}_{\mathrm{Tx(y)}}\right)\right]$$

where $E^{\mathrm{raw}}_{\mathrm{Tx(y)}}$ is the sum over the raw calorimeter tower energies and the jet sum in the equation is over jets with a reconstructed p_{T} above a given jet $p^{\mathrm{cut}}_{\mathrm{T}}$ selection cut, typically

20–25 GeV/c. The jet p_{T} is used in these formula to account for the angular separation of the towers included in the jet sum, contributing to the jet mass. Rewriting the above equation in this form

$$E^{\mathrm{miss}}_{\mathrm{Tx(y)}} = -\big[\big(E^{\mathrm{raw}}_{\mathrm{Tx(y)}} - \sum_{\mathrm{jets}} p^{\mathrm{raw\ jet}}_{\mathrm{Tx(y)}}\big)_{\mathrm{low}\ p_{\mathrm{T}}} + \big(\sum_{\mathrm{jet}} p^{\mathrm{corr.\ jet}}_{\mathrm{Tx(y)}}\big)_{\mathrm{high}\ p_{\mathrm{T}}}\big]$$

shows explicitly the low p_{T} (in the first set of brackets) and the high p_{T} components (second set of brackets) of the MET. The proposed systematics treatment is to vary the components of the low p_{T} MET by 10% scale uncertainty uncorrelated with the high p_{T} component and to vary the high p_{T} component according the jet energy scale uncertainty for the measured jets. If a subset of the high p_{T} jets are identified as electromagnetic objects, isolated electrons or photons, then these EM-jets should be given EM-scale energy corrections which are closer to unity than hadronic jet corrections. The energy scale uncertainty on an EM-object will also be much lower than the jet energy scale systematic. Therefore, if the EM-objects are not removed from the jet list, the quoted energy scale uncertainty will be conservative relative to the lower errors associated with separate treatment of identified EM-objects.

In addition to the jet energy scale uncertainty, there are uncertainties on the jet resolution. At startup the jet resolution is estimated to be accurate to 20% of the quoted resolution based on the test-beam data and simulation studies. The dijet balancing resolution will be determined from data and will further constrain this uncertainty. It is expected that the systematics on the third jet veto and other selection criteria will limit the uncertainty on the jet resolution to 10% in the 1–10 fb^{-1} dataset. The recommended treatment for this systematic is to add an additional smearing to the jet energy which broadens the overall jet resolution by 10%. This can be done by throwing a Gaussian random number and adding an energy term which is 46% of the jet resolution. Therefore, the jet-by-jet event-by-event smearing should be done as follows:

$$E'^{\mathrm{jet}}_{\mathrm{T}} = E^{\mathrm{jet}}_{\mathrm{T}} + \mathrm{Gaus}[0,\ 0.46 * \sigma(E_{\mathrm{T}}, \eta)] \tag{B.9}$$

where $\sigma(E_{\mathrm{T}}, \eta)$ is the reference jet resolution which for the central barrel is given by (using Monte Carlo simulation derived jet calibrations where $E^{\mathrm{MC}}_{\mathrm{T}}$ is equal to $E^{\mathrm{rec}}_{\mathrm{T}}$ on average)

$$\sigma(E^{\mathrm{jet}}_{\mathrm{T}}, |\eta| < 1.4) = (5.8\ \mathrm{GeV}) \oplus \big(1.25 * \sqrt{E^{\mathrm{jet}}_{\mathrm{T}}}\big) \oplus 0.033 * E^{\mathrm{jet}}_{\mathrm{T}} \tag{B.10}$$

(terms added in quadrature) and $\mathrm{Gaus}[0,\ 0.46 * \sigma(E_{\mathrm{T}}, \eta)]$ is a randomly thrown sampling of a normal distribution per jet with a mean of zero and a width of 46% of the jet resolution and therefore $E'^{\mathrm{jet}}_{\mathrm{T}}$ is the smeared jet energy to be used in the estimation of the jet resolution systematic uncertainty of the measurement. The 46% is chosen so that when added in quadrature to the nominal resolution gives an overall widening of the energy resolution of 10%. The resolutions of the endcap and forward jet regions are found in [164, Table 5]. These are

$$\begin{aligned}
\sigma(E^{\mathrm{jet}}_{\mathrm{T}}, 1.4 < |\eta| < 3.0) &= (4.8\,\mathrm{GeV}) \oplus (0.89 * \sqrt{E^{\mathrm{jet}}_{\mathrm{T}}}) \oplus 0.043 * E^{\mathrm{jet}}_{\mathrm{T}} \\
\sigma(E^{\mathrm{jet}}_{\mathrm{T}}, 3.0 < |\eta| < 5.0) &= (3.8\,\mathrm{GeV}) \oplus 0.085 * E^{\mathrm{jet}}_{\mathrm{T}}
\end{aligned}$$

where for these jet resolution fits the stochastic term in the forward region is small compared to the noise and constant terms (hence the missing $\sqrt{E^{\mathrm{jet}}_{\mathrm{T}}}$ term for $3.0 < |\eta| < 5.0$). The shift in the $+10\%$ direction can be symmetrised to account for the -10% shift. Otherwise,

the difference between the reconstructed and generated jet energies must be reduced by 10% in order to estimate the -10% uncertainty from the nominal Monte Carlo jet resolution. The jet resolution uncertainty is particularly important when searching for signals that are on a rapidly falling QCD multi-jet p_{T} spectrum.

B.2.6 Heavy-flavour tagging uncertainties

A strategy for measuring the b-tag efficiency using an enriched sample of b-jets from $\mathrm{t\bar{t}}$ events, and its estimated precision, is described in Section 12.2.8 of [7]. The relative uncertainty on the b-efficiency measurement is expected to be about 6% (4%) in the barrel and 10% (5%) in the endcaps for $1\,\mathrm{fb}^{-1}$ ($10\,\mathrm{fb}^{-1}$) of integrated luminosity. These uncertainties correspond to a b-tag working point efficiency of 50%.

The light-quark (and gluon) mis-tag uncertainty is expected to be larger than the b efficiency uncertainty; however, for this Report a global uncertainty of 5% is assumed for the mis-tag uncertainty. As with the efficiency determination, it is important to identify strategies to measure the mis-tagging probabilities in data as well.

Likewise, a strategy to measure the uncertainty on the efficiency for identifying τ leptons is described in Section 12.1.4 of [7], and involves comparing the ratio of $\mathrm{Z} \to \tau\tau \to \mu{+}\mathrm{jet}$ to $\mathrm{Z} \to \mu\mu$ events. With a $30\,\mathrm{fb}^{-1}$ data sample, the relative uncertainty on τ-tagging is estimated to be about 4%. A measurement of the τ misidentification probability can be determined from a sample of γ+jet events, and with a $10\,\mathrm{fb}^{-1}$ data sample is expected to have an uncertainty at the level of 4–10%.